J. Fluid Mech. (1993), *vol.* 247, *pp.* 231–245

The motion and stability of a vortex array above a pulsed surface

By E. ACTON[1] AND M. R. DHANAK[2]

[1] Asymptote Ltd., St John's Innovation Centre, Cambridge, CB4 4WS, UK

[2] Department of Ocean Engineering, Florida Atlantic University, Boca Raton, FL 33431, USA

(Received 27 June 1991 and in revised form 21 May 1992)

A model inviscid and incompressible flow problem is studied in which an infinite array of equi-spaced identical rectilinear line vortices moves in a uniform stream over a wall in which is embedded an equi-spaced array of discrete line sources of variable strength. It is shown that for a suitable choice of source spacing and strength, a flow that is periodic both in time and in the streamwise direction is possible. The flow is shown to be stable to small two-dimensional disturbances for a range of values of vortex height above the wall and source strength. The implications for the corresponding viscous problem and active flow control are discussed.

1. Introduction

Active control of flow over a surface of a body has been a topic of recent interest: this will generally entail the processes of flow manipulation, pressure monitoring on the body surface and introduction of corrective measures involving, for example, fluid injection and suction through slots on the surface. The flow manipulation may result in structured, somewhat predictive, flow whose effects at the surface may be easier to identify and hence control. However, we expect that the corrective measures in themselves will not only significantly influence the motion of the structured flow but also induce fairly complex secondary flows in the boundary layer. In this paper we consider a canonical inviscid and incompressible problem which involves motion of primary flow structures, organized in the form of an array of spanwise vortices, over a plane rigid surface. For the inviscid problem, the secondary flows are necessarily absent and we examine the effect of a particular type of corrective measure on the motion of the primary flow structures. The problem serves to identify the type of outer 'potential' flow which can arise in the corresponding viscous problem and which can induce possible development of secondary flow in the boundary layer on the plane surface.

Thus we consider the motion and stability of an infinite array of equally spaced, identical vortices in a uniform free-stream flow of an inviscid and incompressible fluid over a plane rigid surface which is embedded with a discrete distribution of line sources whose strengths vary periodically both in time and position along the rigid surface. The vortices are represented by rectilinear line vortices.

In the absence of the embedded sources, the line vortices convect steadily with a speed

$$U = \frac{\aleph}{2\Lambda}\coth\frac{2\pi y_v}{\Lambda} + U_0 \tag{1.1}$$

(Lamb 1932, pp. 225–228), where $\aleph$ is the strength of the vortices, Λ is the

streamwise spacing, y_v is the height of the array above the wall and U_0 is the uniform free-stream speed. The model flow implies a slip speed of $U_0+\aleph/A$ at the rigid surface. The array is, however, unstable to small two-dimensional disturbances, the 'pairing' mode being the most unstable. In this paper we consider the effect of the embedded sources on such an array.

The equations for the model flow are derived in §2, and the basic features of the motion are investigated in §3. It is shown that flows which are periodic both spatially and temporally are possible if the time dependence of the strength of the embedded sources is suitably chosen. In §4, the stability of these periodic flows to infinitesimal two-dimensional disturbances is investigated. It is shown that stable flows are possible for a range of vortex heights above the surface provided that the source strength is suitably pulsed. It is noted that in practice the disturbances may not be small or two-dimensional and it would be necessary to investigate stability to finite three-dimensional disturbances. However, the present stability investigation is a prerequisite for any such consideration.

In the corresponding viscous problem, the vortices in the array may be primary flow structures generated through flow separation, by periodic forcing at a backward-facing spanwise step, for example, at a far upstream location. In this case, the solution obtained here may be regarded as the outer 'potential' flow solution for the viscous boundary layer on the surface. The boundary-layer response to such a potential flow can, in general, be significant. For example, the development of the boundary layer due to the passage of a single spanwise vortex of arbitrary strength over a plane rigid surface leads to production of secondary eddies at the surface (Walker 1978). Similar viscous response to coherent eddies is observed in a turbulent boundary layer (see for example, Smith *et al.* 1991; Falco 1991). In an inviscid model of the kind considered here, any such influence at the wall is characterized by the slip velocity induced at the surface. These characteristics and their implications are considered in §3. It is believed that in the present case, if the induced mean slip velocity is made null through a suitable choice of vortex strength and/or spacing for a given free-stream speed, such an influence may be considerably reduced; the characteristics of the flow in the corresponding viscous problem being significantly different in this case from that of a conventional structured boundary layer. The exact determination of the viscous response will require further investigation.

2. Equations of motion

In this section we obtain the equations which govern the motion of an array of point vortices in an inviscid fluid over a plane wall which is embedded with a discrete distribution of line sources.

We consider the two-dimensional flow in the upper half of (x, y)-plane with the line sources of variable strength equally spaced in the wall along the x-axis (see figure 1). Without loss of generality, we fix the origin to coincide with a source so that the position of the nth source is $(X_n, 0)$ where

$$X_n = na; \quad n = \ldots -3, -2, 0, 1, 2, 3, \ldots, \tag{2.1}$$

where a is the spacing between the sources. The source strengths are taken to be spatially periodic so that if we denote the strength of the nth source by $C_n(t)$, then

$$C_{n+N}(t) = C_n(t), \tag{2.2}$$

so that there are N sources of different instantaneous strengths per spatial

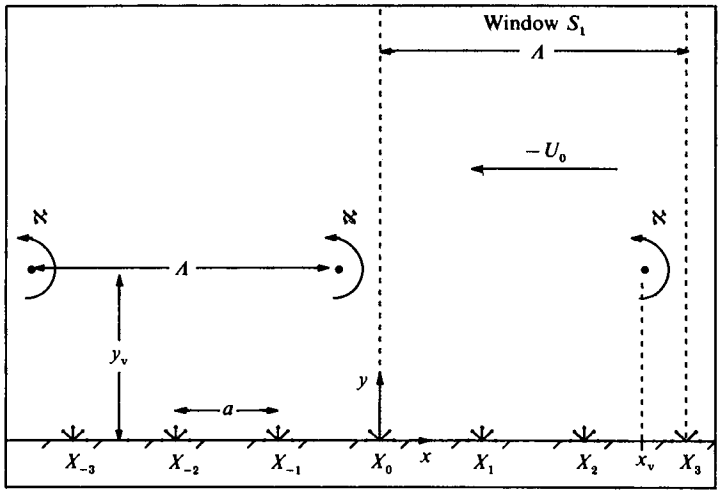

FIGURE 1. Schematic diagram showing the instantaneous position of the equally spaced array of vortices over the wall with sources embedded at $x = X_n$ ($n = \ldots, -2, -1, 0, 1, 2, \ldots$) with $y = 0$. The figure depicts the case with $N = 3$ sources per wavelength. S_1 is a representative window in the spatially periodic array.

wavelength. Thus, in the absence of any vortices in the flow, the instantaneous irrotational velocity at a field point $z = x + iy$, due to the distribution of sources in the rigid wall, can be represented by a complex velocity potential $w_s(z, t)$, where

$$w_s(z,t) = \sum_{n=0}^{N-1} \sum_{m=-\infty}^{\infty} 2C_n(t) \ln(z - X_n - mNa)$$
$$= \sum_{n=0}^{N-1} 2C_n(t) \ln\left\{\sin\left(\frac{\pi}{Na}(z - X_n)\right)\right\}. \tag{2.3}$$

The induced velocity (u_s, v_s) at z is then

$$u_s(x,y,t) - iv_s(x,y,t) = dw_s/dz. \tag{2.4}$$

It may be noted that, except at $x = X_n$ ($n = \ldots -2, 1, 0, 1, 2, \ldots$), the induced normal velocity is zero at the wall and the mass flux per unit spanwise length due to the nth source is $2C_n(t)$. It can be seen from (2.3) that at any given y, the potential is spatially (x) periodic with a wavelength λ_p, such that λ_p is an integral multiple of Na, that is

$$\lambda_p = p(Na), \quad p \text{ an integer}. \tag{2.5}$$

We now suppose that the flow field consists of an infinite linear array of point vortices of equal strength $\aleph$ and spacing Λ supported in a uniform stream U_0 over the wall. Then the instantaneous complex potential for the irrotational velocity at a field point z is given by

$$w(z,t) = \frac{\aleph}{2\pi i} \ln\left\{\frac{\sin[(\pi/\Lambda)(z - z_{v0})]}{\sin[(\pi/\Lambda)(z - z_{v0}^*)]}\right\} + w_s(z,t) + U_0 z + \text{constant}, \tag{2.6}$$

where z_{v0} denotes the position of a vortex in the array, the asterisk denotes complex conjugate and w_s is given by (2.3).

The expression (2.6) for the velocity potential holds provided that the point vortices are maintained as a linear array. However, a point vortex moves with the

velocity induced at the point by external sources; thus the position of the mth vortex is governed by

$$\frac{\mathrm{d}z^*_{vm}}{\mathrm{d}t} = \frac{\aleph}{2\pi \mathrm{i}}\left\{ \sum_{\substack{n \\ n \neq m}} \frac{1}{z_{vm}-z_{vn}} - \sum_n \frac{1}{z_{vm}-z^*_{vn}} \right\} + \left.\frac{\mathrm{d}w_s}{\mathrm{d}z}\right|_{z=z_{vm}} + U_0, \tag{2.7}$$

where
$$z_{vp} = z_{v0} + p\Lambda \quad (p = \ldots -2, -1, 0, 1, 2, \ldots). \tag{2.8}$$

In the absence of the source distribution on the plane wall ($w_s \equiv 0$), each vortex over the wall experiences the same velocity and therefore moves in unison with other vortices so that they are maintained as a linear array. This property still holds when the source distribution on the wall is present (with w_s given by (2.3)), provided that

$$\Lambda = \lambda_p = p(Na), \quad p \text{ an integer} \tag{2.9}$$

from (2.5); that is, Λ is an integral multiple of the wavelength associated with the source distribution on the wall. It is then only necessary to follow the motion of one vortex in the array, z_0 say, and use (2.8) to determine the position of the other vortices.

We choose to study only the case $p = 1$ in detail so that the flow field is then spatially (x) periodic with wavelength Λ and for every vortex in the array there are N line sources on the wall. Thus the flow field can be divided into sections or windows of length Λ and the flow need be evaluated in only one such section.

We choose to consider the flow in the window S_1 defined by $0 \leqslant x < \Lambda$ so that, in view of (2.1), the line sources along the wall in S_1 are at $(X_n, 0)$ $n = 0, 1, 2, \ldots, N-1$, where $X_n = n\Lambda/N$. In view of (2.2), the strength of the sources at $(X_0, 0)$ and at $(X_N, 0)$ in the adjacent window S_2 is $C_0(t)$. Suppose that at a given instant the mth vortex in the array is in the window S_1 at the position $z_{vm} = z_v$. Then it follows from (2.3), (2.6) and (2.9) that the instantaneous complex velocity potential at a field point z is given by

$$w(z,t) = \frac{\aleph}{2\pi \mathrm{i}} \ln\left\{ \frac{\sin(\frac{1}{2}K(z-z_v))}{\sin(\frac{1}{2}K(z-z^*_v))} \right\} + \sum_{n=0}^{N-1} \frac{C_n(t)}{\pi} \ln\{\sin(\tfrac{1}{2}K(z-X_n))\} + U_0 z, \tag{2.10}$$

where $K = 2\pi/\Lambda$; the arbitrary constant in (2.6) is here set to zero. The instantaneous velocity (u, v) at z is given by

$$u(x,y,t) - \mathrm{i}v(x,y,t) = \mathrm{d}w/\mathrm{d}z. \tag{2.11}$$

We obtain the equations governing the position $z_v(t)\,(= x_v(t) + \mathrm{i}y_v(t))$ of the vortex in the window S_1 on substituting (2.4) and (2.8) into (2.7) and using (2.9). Thus after evaluating the sum in (2.7), we have for $y_v > 0$,

$$\frac{\mathrm{d}x_v}{\mathrm{d}t} = \frac{\aleph}{2\Lambda}\coth Ky_v + \frac{1}{\Lambda}\sum_{n=0}^{N-1} \frac{C_n(t)\sin Ks_n}{\cosh Ky_v - \cos Ks_n} + U_0, \tag{2.12}$$

$$\frac{\mathrm{d}y_v}{\mathrm{d}t} = \frac{1}{\Lambda}\sum_{n=0}^{N-1} \frac{C_n(t)\sinh Ks_n}{\cosh Ky_v - \cos Ks_n}, \tag{2.13}$$

where
$$s_n(t) = x_v(t) - X_n = x_v(t) - n\Lambda/N. \tag{2.14}$$

The positions of the vortices in the adjacent windows are given by

$$z_{v(m\pm1)} = z_v \pm \Lambda. \tag{2.15}$$

Thus if the mth vortex traverses into an adjacent window, $z_v \pm \Lambda$ gives the position of the vortex which has traversed into the window S_1.

The slip velocity at the wall surface is given by

$$u(x,t) = U_0 + \frac{\aleph}{\Lambda}\left(\frac{\sin Ky_v}{\cosh Ky_v - \cos K(x-x_v)}\right) + \frac{1}{\Lambda}\sum_{n=0}^{N-1} C_n(t)\cot\tfrac{1}{2}K(x-X_n), \quad (2.16)$$

the mean value, $\bar{u}$, being $U_0+\aleph/\Lambda$; the last term on the right-hand side has singularities at $x = X_n$ and $\bar{u}$ is obtained as a Cauchy principal value of the relevant integral.

Equations (2.10)–(2.13) suffice to describe the instantaneous flow field and can be used to follow the motion from a given initial position of the vortex in S_1 for a prescribed source strength variation $C_n(t)$. The case when the source strength is constant in time is briefly considered in the Appendix. However, the case where the sources are of variable strength is of interest here and this is pursued in detail in the following sections.

3. Basic features of the flow

We consider a particular, periodically varying, source strength,

$$C_n(t) = -C_0\cos(Ks_n + \phi); \quad -\pi < \phi \leqslant \pi, \quad (3.1)$$

where $s_n(t)$ is given by (2.14) and defines the position of the vortex in a window relative to the nth source in that window; and where both ϕ, the phase of the wave relative to the vortex, and C_0, its amplitude, are held constant. The flow associated with this choice of $C_n(t)$ corresponds to that over a virtual surface in the form of a travelling wave at the wall which maintains its phase relative to the streamwise position of the vortex array. $C_n(t)$ is plotted as a function of n/N in figure 2 for the case when there are $N = 6$ sources in the window, at a fixed time $t = t_0$. Four cases are shown with the phase set to $\phi = 0$, $\pm\frac{1}{2}\pi$ and π. In each, the smooth line joining the discrete points defines the virtual surface. With the source strength defined according to (3.1), the virtual surface always has the same form relative to the instantaneous position of the vortex; effectively, the motion at the wall is 'tuned' or locked in to the motion of the vortex.

The corresponding motion of the vortex array is calculated by integrating (2.12) and (2.13) using a fourth-order Runge–Kutta scheme. Results are presented for a particular choice of the vortex strength,

$$\aleph/\Lambda = -U_0. \quad (3.2)$$

It is shown in the Appendix that when $\phi \neq \pm\frac{1}{2}\pi$, the vortices have a non-zero mean velocity normal to the wall so that the motion is not periodic and the vortices drift towards or away from the wall. When $\phi = \pm\frac{1}{2}\pi$, the normal velocity has a zero mean and the motion is periodic. The mean streamwise velocity is faster or slower than that given by (1.1) according to whether $\phi = +\frac{1}{2}\pi$ or $\phi = -\frac{1}{2}\pi$.

Here, we restrict consideration to the periodic cases corresponding to $\phi = \pm\frac{1}{2}\pi$. However, as discussed in the next section, stable solutions are possible only for $\phi = -\frac{1}{2}\pi$. We therefore present detailed results for this value of ϕ; the differences in the vortex paths for given initial conditions and source strength between $\phi = \pm\frac{1}{2}\pi$ are illustrated in figure 3.

It may be noted that with the choice (3.1) for $C_n(t)$, the system (2.12)–(2.14) is autonomous. Further, the right-hand side of (2.12) and (2.13) are continuously differentiable with respect to x_v and $y_v > 0$. Thus by the existence and uniqueness theorem of differential equations, any initial condition $x_v(0) = a_1$, $y_v(0) = a_2$ gives rise to a unique trajectory through the point (a_1, a_2) so that any two trajectories

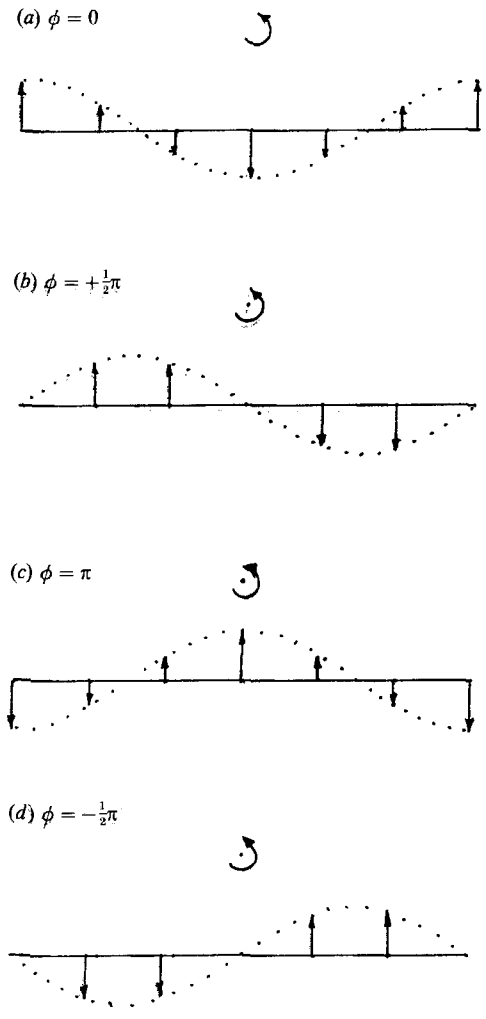

FIGURE 2. Possible forms, relative to the vortex, of the virtual surface at the wall associated with source strength $C_n(t)$ given by (3.1) with (*a*) $\phi = 0$, (*b*) $\phi = \frac{1}{2}\pi$, (*c*) $\phi = \pi$ and (*d*) $\phi = -\frac{1}{2}\pi$. The figure depicts the form of the wave defined by instantaneous strength of sources for the case of $N = 6$ sources per wavelength.

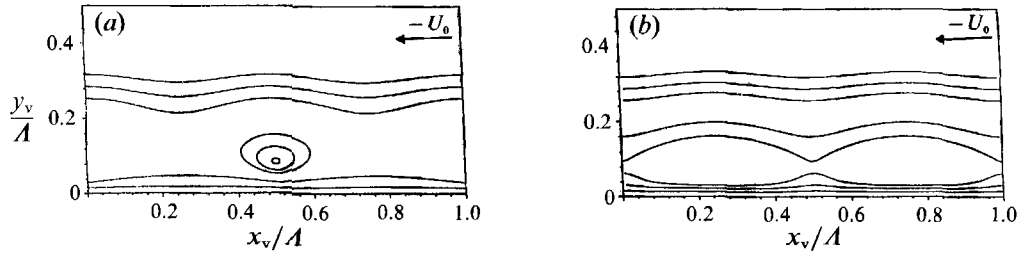

FIGURE 3. Contrast between vortex paths corresponding to phase (*a*), $\phi = \frac{1}{2}\pi$ and (*b*) $\phi = -\frac{1}{2}\pi$. The source strength amplitude is $\epsilon_0 = 0.2$ and $N = 2$. The solid curves shown are trajectories of the vortices in a representative window S_1.

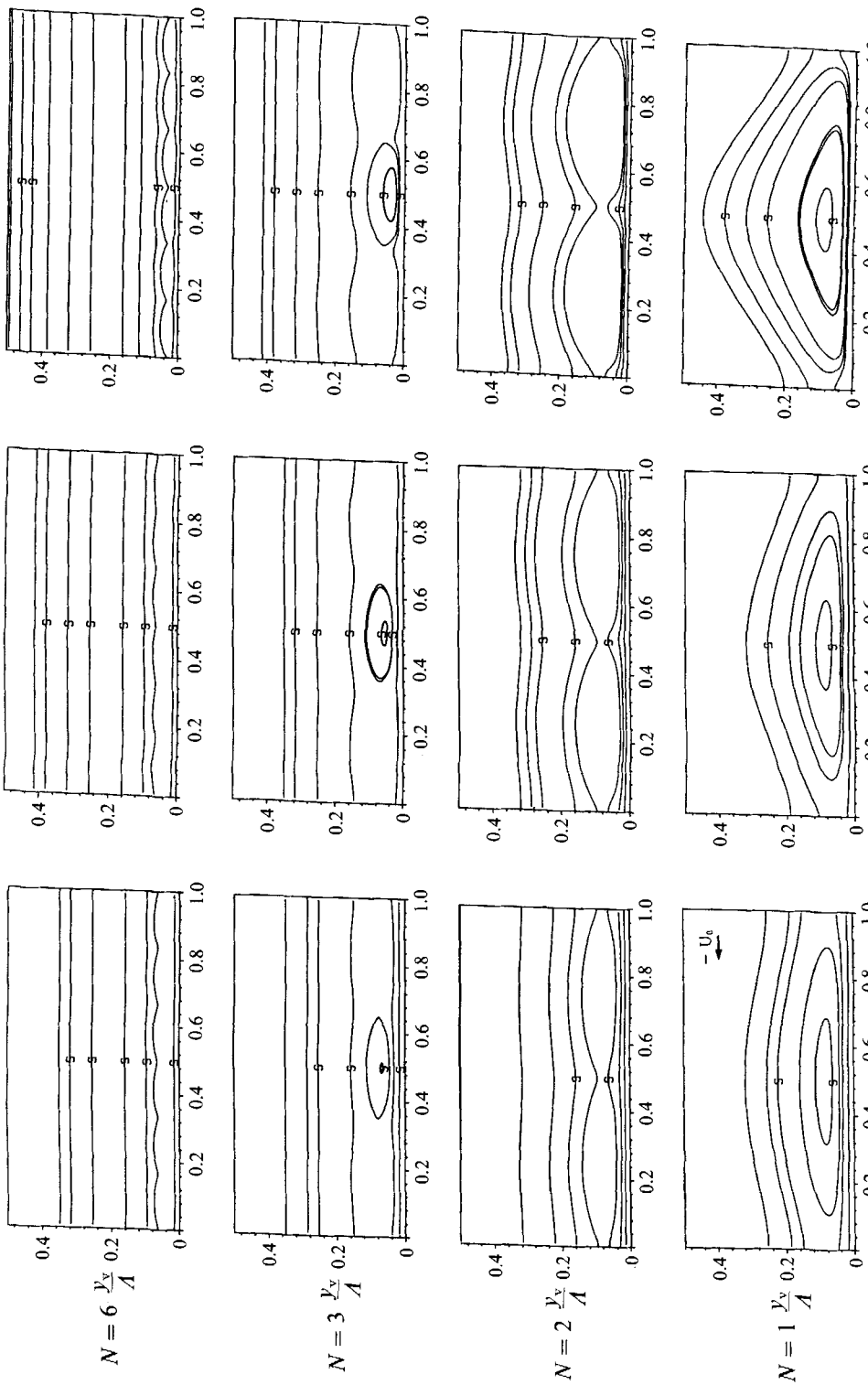

FIGURE 4. Vortex paths corresponding to various values of N, number of sources per wavelength, and source strength amplitude, ϵ_0. The curves shown in each part are trajectories of the vortices in a representative window S_1. The direction of the free stream is from right to left. Paths marked with letter S indicate stable paths; those left unmarked are unstable.

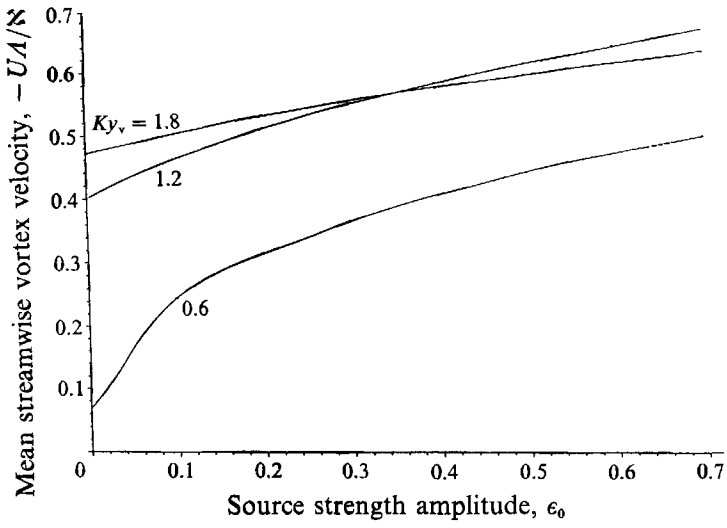

FIGURE 5. Variation of mean streamwise vortex velocity with source strength amplitude for three values of instantaneous vortex height corresponding to position $Kx_v = \pi$. The streamwise direction is along the negative x-axis (see figure 1).

cannot cross. The values of the pair (x_v, y_v) for which the right-hand sides of (2.12) and (2.13) both vanish are the critical points of the system for which the trajectories are degenerate and are just points. For N sources per window in the wall, there are N critical points in the window. When $\phi = \pm\frac{1}{2}\pi$, these critical points are centres; that is, trajectories close to the critical points form closed orbits.

The vortex paths with different discrete source conditions at the wall are shown in figure 4 for various initial positions of the vortex array. In all cases shown, the vortex in the window is initially positioned at $x_v/\Lambda = 0.5$ whilst the initial height of the array above the wall is varied. In the chosen window the sources are positioned along the wall according to (2.14) at $X_n = n\Lambda/N$, where $n = 0, 1, \ldots, N-1$. Figure 4 shows the paths for the number of sources per window, $N = 1$, 2, 3 and 6, and for three values of the source amplitude, $\epsilon_0 = 0.1$, 0.2 and 0.4, where $\epsilon_0 = C_0\pi/\aleph$. The free-stream direction is from right to left. When the array is positioned close to the wall, the vortices move upstream as indicated earlier. If the array is positioned further out from the wall the vortices may move in closed paths. With the initial value of $x_v/\Lambda = 0.5$ chosen here, closed paths are possible only when there is an odd number N of sources per window, that is when each vortex is not initially above a source; this is because with N odd, $x_v/\Lambda = 0.5$ is midway between two sources. However, when the vortex array is initially positioned sufficiently far from the wall, the vortices move in the direction of the free stream. In this case, when each vortex periodically traverses the length of the window section in time T, then a frequency $\omega_0 = 2\pi/T$ is implied by the motion. This suggests that $C_n(t)$ can alternatively be of the form

$$C_n(t) = -C_0 \cos(\omega_0 t - 2\pi n/N + \phi),$$

where the sign of the phase $2\pi n/N$ ensures that the wave moves in the direction of the free stream. This definition of $C_n(t)$ corresponds to a surface that is controlled externally rather than one, as given by (3.1), which is 'tuned' or locked in to the flow.

The mean velocity of the vortex array is given by $\bar{U} = \Lambda/T = \Lambda\omega_0/2\pi$. It is shown in the Appendix that as the source strength ϵ_0 is increased the vortex array moves

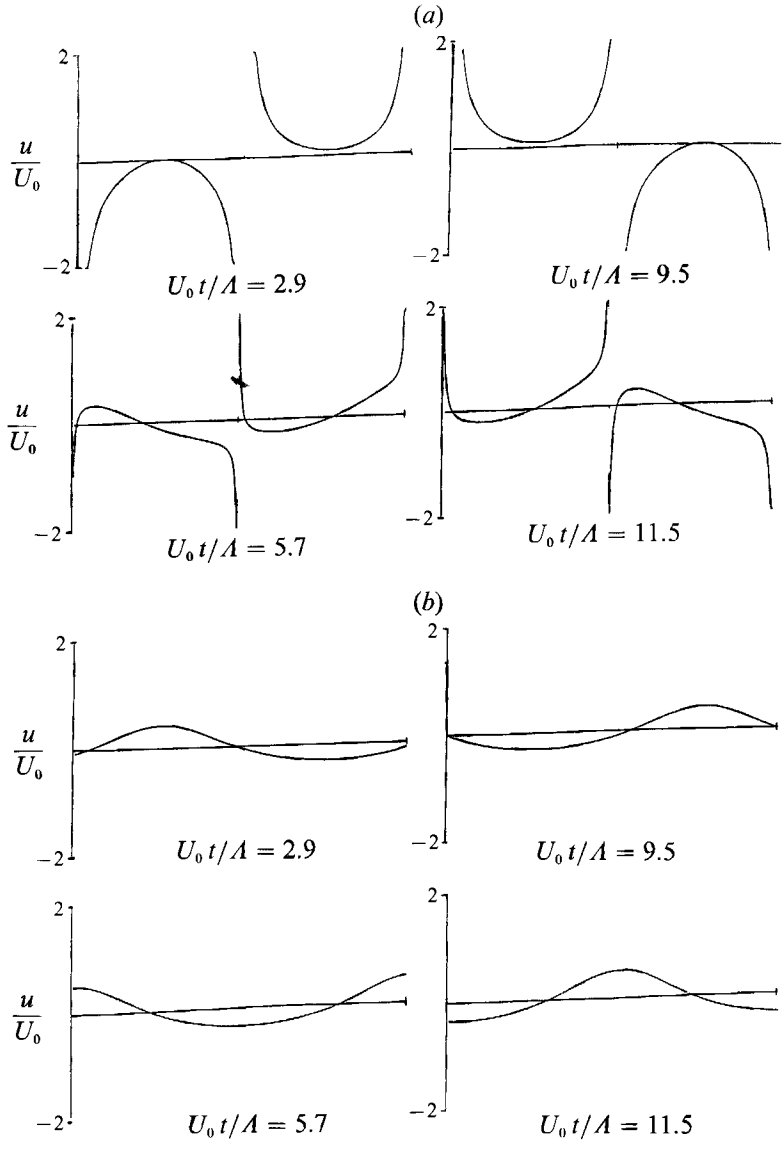

FIGURE 6. A comparison of instantaneous slip velocity at the wall between case (*a*) with $N = 2$ sources embedded in the wall, $\epsilon_0 = 0.2$ and with the vortex in the window initially positioned at $Kx_v = \pi$, $Ky_v = 1.6$; and case (*b*) with no sources embedded in the wall. The slip velocity is plotted against x/Λ.

with a higher mean speed; figure 5 shows this variation in mean speed with source strength for $N = 2$ as the initial vortex position is altered.

In an inviscid model flow of the type considered here, the slip velocity at the plane surface governs the pressure gradient in the boundary layer at the wall surface in the corresponding viscous problem. The slip velocity given by (2.16) is shown in figure 6 for a particular case. In this model problem, the slip velocity has singularities at the location of the sources although, with the choice (3.2), its mean value is zero; in practice, with finite-size suction slots, the velocity will have finite peak values in the vicinity of the source locations.

In general, the presence of coherent vortices near a wall can induce a significant viscous response at the wall surface. Walker (1978), for example, has evaluated the response in the case of a single spanwise eddy in steady motion over a plane surface: in a frame of reference moving with the vortex (so that the mean slip velocity at the surface in the associated inviscid problem is $-3\aleph/4\pi h$, where h is the vortex height), counter eddies are observed to form at the surface. Similar viscous response is observed in a turbulent boundary layer due to the presence of coherent eddies in its outer layer (Smith *et al.* 1991; Falco 1991). In the present problem, such a response has not been determined. In view of the chosen condition (3.2), the mean velocity gradient and the mean pressure gradient in the boundary layer at the wall, in the corresponding viscous problem, are expected to be small. It is believed that this will minimize the unsteady development of the boundary layer of the type suggested by Walker. This belief is based on experimental observations, of Uzkan & Reynolds (1967) for example, that turbulence production in a boundary layer is inhibited if the wall surface beneath the boundary layer is made to move with the mean streamwise velocity. It is possible that the presence of local peaks in the pressure gradient associated with the source flow may still have significant effects; however, in considering such effects, it must be borne in mind that the pressure peaks are transient for the periodically varying source strength. Thus the exact viscous response for the present problem remains to be determined.

4. Stability of the linear array of vortices

We examine the stability of the vortex motion, and hence the associated inviscid flow considered in §3, to small two-dimensional disturbances in the flow. It is noted that in practice the disturbances present may not be small nor two-dimensional and the present investigation needs to be supplemented by a further study if finiteness and the three-dimensional nature of the disturbances are both investigated. The determination of the stability to small two-dimensional disturbances is however a prerequisite for any such study.

We suppose that each vortex in the array is perturbed from its quasi-steady path by plane infinitesimal disturbances which do not bend the vortex lines. Let the instantaneous perturbed position of the mth vortex in the array be given by

$$z_{vm} = \hat{z}_{vm}(t) + \epsilon \tilde{z}_{vm}(t); \quad \hat{z}_{vm} = z_v(t) + mA, \tag{4.1}$$

where $\epsilon \ll 1$ and $z_v(t)\,(= x_v(t) + iy_v(t))$ satisfies (2.12)–(2.13) for the unperturbed flow. The unsteady basic flow is considered to be stable if the perturbations which are bounded initially remain bounded for all time.

On substituting (4.1) into (2.7) we have

$$\frac{d\hat{z}^*_{vm}}{dt} + \epsilon \frac{d\tilde{z}^*_{vm}}{dt} = \frac{\aleph}{2\pi i}\left\{ \sum_{\substack{n \\ n \neq m}} \frac{\left(1 + \epsilon \dfrac{(z_{vm} - z_{vn})}{(m-n)A}\right)^{-1}}{(m-n)A} - \sum_{n} \frac{\left(1 + \epsilon \dfrac{(z_{vm} - z_{vn})}{(m-n)A + 2iy_v}\right)^{-1}}{(m-n)A + 2iy_v} \right\}$$
$$+ \left.\frac{dw_s}{dz}\right|_{z = \hat{z}_{vm} + \epsilon \tilde{z}_{vm}} + U_0. \tag{4.2}$$

Then expanding the right-hand side of (4.2) in terms of ϵ we find that whilst the terms

independent of e are satisfied identically in view of (2.12)–(2.13), the terms proportional to e give

$$\frac{\mathrm{d}\tilde{z}^*_{vm}}{\mathrm{d}t} = \frac{\aleph}{2\pi \mathrm{i} A^2}\left\{\sum_{\substack{n\\ n\neq m}} \frac{\tilde{z}_{vm}-\tilde{z}_{vn}}{(m-n)^2} - \sum_n \frac{((m-n)-\mathrm{i}k)^2}{((m-n)^2+k^2)^2}(\tilde{z}_{vm}-\tilde{z}_{vn})\right\} + \tilde{z}_{vm}\frac{\mathrm{d}^2 w_s}{\mathrm{d}z^2}\bigg|_{z=z_v}, \quad (4.3)$$

where $k = 2y_v/A$. We proceed with the stability analysis following Lamb (1932, p. 226): we write $\tilde{z}_{vm} = \tilde{x}_{vm} + \mathrm{i}\tilde{y}_{vm}$, separate the real and imaginary parts of (4.3) and look for solutions of the form

$$\tilde{x}_{vm}(t) = \tilde{X}(t)\,\mathrm{e}^{\mathrm{i}m\psi}, \quad \tilde{y}_{vm}(t) = \tilde{Y}(t)\,\mathrm{e}^{\mathrm{i}m\psi}; \quad 0 \leqslant \psi \leqslant 2\pi. \quad (4.4)$$

We find that $\tilde{X}, \tilde{Y}$ are given by

$$(\tilde{X}, \tilde{Y}) = (X(t), Y(t))\exp\left(\mathrm{i}\int_0^t B(t)\,\mathrm{d}t\right), \quad (4.5)$$

where X, Y satisfy

$$\frac{A^2}{\aleph}\frac{\mathrm{d}X}{\mathrm{d}t} = -(A+2\pi P-C)\,Y - 2\pi Q X, \quad \frac{A^2}{\aleph}\frac{\mathrm{d}Y}{\mathrm{d}t} = -(A+2\pi P-C)\,X - 2\pi Q Y, \quad (4.6)$$

with

$$P(t) = \sum_{n=0}^{N-1} \frac{C_n(t)\sin Ks_n \sinh Ky_v}{\aleph(\cosh Ky_v - \cos Ks_n)^2}; \quad Q(t) = \sum_{n=0}^{N-1} \frac{C_n(t)(1-\cos Ks_n \cosh Ky_v)}{\aleph(\cosh Ky_v - \cos Ks_n)^2},$$

$$A = \frac{1}{2\pi}\left\{\sum_{\substack{n\\ n\neq m}} \frac{1-\mathrm{e}^{\mathrm{i}m\psi}}{n^2} - \sum_n \frac{n^2-k^2}{(n^2+k^2)^2}\right\} = \frac{1}{4\pi}\left(\psi(2\pi-\psi) + \frac{2\pi^2}{\sinh^2 \pi k}\right),$$

$$B = \frac{1}{\pi}\sum_n \frac{nk\sin n\psi}{(n^2+k^2)^2} = \frac{1}{2}\left(\frac{\pi\psi\cosh k(\pi-\psi)}{\sinh k\pi} - \frac{\pi^2 \sinh k\psi}{\sinh^2 \pi k}\right),$$

$$C = \frac{1}{2\pi}\sum_n \frac{(n^2-k^2)\,\mathrm{e}^{\mathrm{i}n\psi}}{(n^2+k^2)^2} = -\frac{1}{2}\left(\frac{\psi \sinh k(\pi-\psi)}{\sinh k\pi} - \frac{\pi\cosh k\psi}{\sinh^2 \pi k}\right),$$

and $s_n = x_v - X_n$. For periodic motion of the vortices, determined by (2.12)–(2.13) with appropriate choice of $C_n(t)$ and U_0, the coefficients of the coupled equations (4.6) are periodic with the same period T as that associated with the motion of the vortices. Further, the coefficients have no singularities for $y_2 > 0$. Thus the nature of the solutions to (4.6) may be established by Floquet theory (Ince 1956, p. 381). The theory determines whether (4.6) admit solutions which grow in time. If they do, then the vortex path being considered is not stable.

Equation (4.6) (together with (2.12)–(2.13)) is integrated over a period with initial conditions

$$X^{(1)}(0) = 1, \quad Y^{(1)}(0) = 0 \quad \text{and} \quad X^{(2)}(0) = 0, \quad Y^{(2)} = 1 \quad (4.7)$$

respectively and given initial values of (x_v, y_v) using a fourth-order Runge–Kutta method; the superscripts are used to distinguish the two solutions. Then the nature of any solution to (4.6) is determined by the eigenvalues of the non-singular matrix,

$$\boldsymbol{D} = \begin{pmatrix} X^{(1)}(T) & X^{(2)}(T) \\ Y^{(1)}(T) & Y^{(2)}(T) \end{pmatrix}$$

If the two eigenvalues of $\boldsymbol{D}$ are not distinct, the system (4.6) admits a solution which

grows, at least linearly in time. If the eigenvalues are distinct, any solution of (4.6) can be written

$$X(t) = A_0 e^{\mu_1 t} F_{\mu_1}(t) + B_0 e^{\mu_2 t} F_{\mu_2}(t), \quad Y(t) = A_0 e^{\mu_1 t} G_{\mu_1}(t) + B_0 e^{\mu_2 t} G_{\mu_2}(t),$$

where $\hat{\lambda}_i = e^{\mu_i T}$ are the eigenvalues of $\boldsymbol{D}$, $F_{\mu_i}(t)$ and $G_{\mu_i}(t)$ are periodic with period T and A_0 and B_0 are constants. If the real part of either characteristic exponent μ_i is positive, the system (4.6) admits solutions which grow exponentially in time. Thus for stability we require that the eigenvalues of the matrix $\boldsymbol{D}$ be distinct and that each μ_i satisfy $\mathrm{Re}(\mu_i) \leqslant 0$.

Since in (4.6), A, P, Q and C are symmetric in ψ about $\psi = \pi$, the stability characteristics will be symmetric about $\psi = \pi$. Thus it is sufficient to study the case $0 \leqslant \psi \leqslant \pi$.

The stability characteristics were investigated for the basic vortex paths defined by (2.12)–(2.13) with condition (3.2) and source strength $C_n(t)$ given by (3.1) with phase $\phi = \pm\frac{1}{2}\pi$. No stable solutions were found over the range of parameter space considered for $\phi = +\frac{1}{2}\pi$. A possible qualitative explanation for this is afforded by the illustration in figure 2(*b*). The figure shows the position of the vortex in a window in relation to the virtual surface underneath. If the vortex is perturbed upwards (downwards) from this position, its streamwise speed will increase (decrease) so that the vortex will be over an instantaneous source (sink) which will enhance its upward (downward) shift. Thus the perturbations will grow. This does not happen when $\phi = -\frac{1}{2}\pi$ (figure 2*d*): a small upward (downward) shift of the vortex from its unperturbed position and the subsequent increase (decrease) in its streamwise speed imply that the vortex will be over an instantaneous sink (source) which will oppose its upward (downward) motion. Thus it is possible that the growth of the disturbances is checked for a range of flow parameters so that stable vortex paths exist for $\phi = -\frac{1}{2}\pi$. Henceforth, we therefore restrict attention to that case only and show that stable vortex paths indeed exist for this case.

An extensive search revealed that the least stable mode of disturbances is the 'pairing mode', which corresponds to $\psi = \pi$ in (4.4). This result is consistent with the corresponding result for the array in the absence of the source distribution. It is thus only necessary to consider perturbations corresponding to $\psi = \pi$ in order to determine the stability of a vortex path. The parametric results below are based on this criterion.

For the number of sources per window, $N = 1$, 2, 3 and 6, the perturbed vortex paths corresponding to a range of values of the source strength amplitude C_0 and a range of values of initial vortex heights were considered. The initial streamwise position of the unperturbed vortex was taken to be $x_v = \frac{1}{2}\Lambda$. The stability boundaries are shown in figure 7(*a–d*) where the initial vortex height $y_v(0)/\Lambda$ is plotted against the source strength $\epsilon_0 = \pi C_0/\aleph$. In the figures, stability refers to neutral stability with respect to infinitesimal disturbances.

Close to the wall, where in their unperturbed state the vortices travel upstream or in closed paths, the stability boundaries are difficult to define accurately and are tentatively drawn in the figures by enclosing points which correspond to stable vortex paths. The boundaries consist of a number of branches enclosing regions of stability in the $(y_v(0)/\Lambda, \epsilon_0)$-plane. The branches become less numerous as N is increased.

Further away from the wall, it is possible to identify the stability boundaries more accurately. Typically they consist of two branch curves such that the region between the curves corresponds to stable vortex paths. Figure 7(*a*) illustrates the case of one

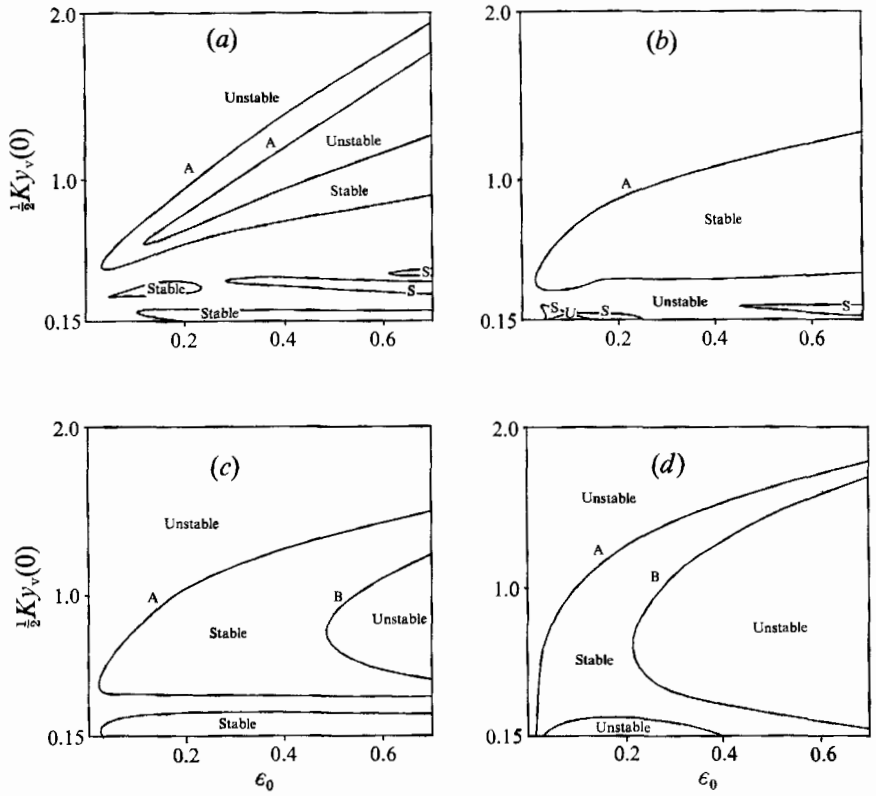

FIGURE 7. Stability boundaries for periodic flows with N sources per wavelength embedded in the wall: (*a*) $N = 1$, (*b*) $N = 2$, (*c*) $N = 3$ and (*d*) $N = 6$.

source per window ($N = 1$). This case is different from the others considered in that the corresponding virtual surface (cf. §3) at the wall is not wavy. The stability characteristics are accordingly somewhat different in this case although the stability boundaries still consist of two branches, marked respectively A and A′. The stable region is enclosed between the two branches. Thus for $0.04 \lesssim \epsilon_0 \lesssim 0.13$, and $y_v(0)/\Lambda > 0.45/\pi$ the range of stable vortex heights increase with ϵ_0. For $\epsilon_0 \gtrsim 0.13$ and $y_v(0)/\Lambda > 0.55/\pi$, for each ϵ_0 there are two narrow ranges of stable vortex heights, separated by a range of unstable heights.

Branch A of the stability boundary is a common feature for other values of N also. Apparently, the relevant parameter is $N\epsilon_0$, the root-mean-square value of the instantaneous volume flux at the wall. The left-most point on Branch A corresponds to $N\epsilon_0 \approx 0.04$. The branch widens out for $\epsilon_0 \gtrsim 0.04/N$, the width for a given ϵ_0 increasing with N. Branch A′ of the stability boundary which is a feature of the $N = 1$ case has no counterpart for $N > 1$. However, there is a second branch B which lies to the right of $\epsilon_0 \gtrsim 1.44/N$ and which is completely enclosed by branch A. Branch B also widens out for $\epsilon_0 \gtrsim 1.44/N$.

Figure 7 (*b*) depicts the case $N = 2$ and shows Branch A of the stability boundary. The ordinate $\epsilon_0 = 1.44/N$ lies to the right of the range of ϵ_0 shown so that Branch B of the stability boundary does not appear in the figure. Thus in the range of ϵ_0 shown, the range of stable vortex heights for $y_v(0)/\Lambda > 0.35/\pi$ increases with ϵ_0. Note that for the initial position $x_v = \frac{1}{2}\Lambda$, there are no closed paths for this case. The feature of the stability characteristics represented by Branch B of the boundary is shown for

$N = 3$ and 6 in figures 7 (*c*) and 7 (*d*) respectively. For $0.04 \gtrsim N\epsilon_0 \gtrsim 1.44$, the range of stable vortex heights increases with ϵ_0 as for $N = 2$. For $\epsilon_0 \gtrsim 1.44$, for each ϵ_0 there are two narrow ranges of vortex heights at which the array is stable. The width of the two ranges becomes smaller as ϵ_0 is increased while the width of the unstable region separating the two ranges becomes bigger.

The stable vortex paths in figure 4 are denoted by 'S' while those which are unstable are left unmarked. It may be noted that for small values of ϵ_0 the range of stable vortex heights increases with N while for each fixed N, the range of stable vortex heights increases with ϵ_0. This is evident from figure 7 (*a–d*). When ϵ_0 is as large as 0.4, the stable range still increases with N and ϵ_0 respectively for $N \leqslant 3$. However, for $N = 6$ the stable paths corresponds to two narrow ranges of vortex heights separated by a large range of heights for which the vortex paths are unstable. As may be seen from figure 7 (*d*), the latter corresponds to the unstable region enclosed by Branch B of the stability boundary. It may also be noted from figure 4 that some of the closed paths are also stable.

5. Conclusions

We have shown that for an array of vortices over a plane surface embedded with sources of variable strength, periodic flows are possible if the vortex array spacing is an integer multiple of the source array spacing and if the source strength varies periodically with a constant phase with respect to the moving array. The instantaneous strength of a source varies according to its position along the wall in such a way as to define a virtual surface which is in the form of a travelling wave at the wall. Typical periodic paths are shown in figure 4 for $N = 1$, 2, 3 and 6 and for three values of the source strength amplitude. For a range of the source strength amplitude and array height above the wall, it is shown that periodic flows which are stable to small, two-dimensional disturbances are possible. Thus the present model suggests that an array of vortices in an inviscid fluid can stably persist over a plane surface if a suitable oscillating volume flux is introduced at the surface. Stable flows have been shown to exist for the case where the mean slip velocity is zero so that the characteristics of the flow in the corresponding viscous problem may be significantly different from that of a conventional boundary layer, leading to the interesting possibility of a considerably reduced viscous response to the presence of the array. However, the problem of the viscous response requires further investigation.

The paper is based on work carried out by the authors while they were at Topexpress Ltd., Cambridge and was partially supported by Rolls Royce plc.

Appendix. Choice of source strength

It can be shown that the vortex velocity given by (2.12)–(2.14) can be written in a series form as

$$\frac{\mathrm{d}x_\mathrm{v}}{\mathrm{d}t} = U + K \sum_{n=0}^{N-1} \frac{C_n(t) \sin Ks_n}{\sinh Ky_\mathrm{v}} Q(Ky_\mathrm{v}, s_n); \quad \frac{\mathrm{d}y_\mathrm{v}}{\mathrm{d}t} = K \sum_{n=1}^{N-1} C_n(t)\, Q(Ky_\mathrm{v}, s_n), \quad \text{(A 1)}$$

where U is given by (1.1) and

$$Q = \left(1 + 2 \sum_{m=1}^{\infty} \mathrm{e}^{-mKy_\mathrm{v}} \cos mKs_n\right).$$

For $C_n(t)$ given by (3.2), these become

$$\frac{\mathrm{d}x_\mathrm{v}}{\mathrm{d}t} = U - \frac{KC_0}{2\sinh Ky_\mathrm{v}} \sum_{n=0}^{N-1} \{F(t)\sin(2Ks_n+\phi) - Q\sin\phi\}, \tag{A 2}$$

$$\frac{\mathrm{d}y_\mathrm{v}}{\mathrm{d}t} = -\tfrac{1}{2}KC_0N\{\mathrm{e}^{-Ky_\mathrm{v}}\cos\phi + \delta_{1N}\cos(Ks_0+\phi) + (\delta_{1N}+\delta_{2N})\,\mathrm{e}^{-2Ky_\mathrm{v}}\cos(2Ks_0+\phi) + H_+ + H_-\}, \tag{A 3}$$

where $\delta_{ij} = 1$ if $i = j$, $\delta_{ij} = 0$ if $i \neq j$,

$$F_n(t) = 1 + \sum_{m=1}^{\infty} \mathrm{e}^{-mKy_\mathrm{v}} \sin((m+2)Ks_n + \phi)$$

and

$$H_\pm = \sum_{\substack{m=2 \\ m\pm1 \equiv N}}^{\infty} \mathrm{e}^{-mKy_\mathrm{v}} \cos m(K(m\pm1)s_0 + \phi).$$

We note that the first term on the right of (A 3) is non-oscillatory and it can be shown that for $N \geqslant 2$, the vortex height is of the form

$$Ky_\mathrm{v} = \ln(\beta - \tfrac{1}{2}K^2C_0Nt\cos\phi) + G(t), \tag{A 4}$$

where $G(t)$ is an oscillatory function with zero mean and β is a constant. Thus if $\phi \neq \pm\frac{1}{2}\pi$ the vortex height will increase or decrease logarithmically according as $|\phi| > \frac{1}{2}\pi$ or $|\phi| < \frac{1}{2}\pi$ and the flow will not be periodic in time. However, if $\phi = \pm\frac{1}{2}\pi$, although (A 2) implies that there will be a net increase or decrease in the mean streamwise velocity, the flow will be periodic in time. A similar result holds for the case $N = 1$.

It may be noted that if the source strength does not vary in time and is of the form

$$C_n(t) \equiv -\tfrac{1}{2}C_0\cos(K(s_0 + n/N) + \phi) \quad n = 0, 1, 2, \ldots, N-1, \tag{A 5}$$

then the vortex paths are given by the $\mathrm{Im}(W_1(z)) \equiv$ constant, where $W_1(z)$ is the complex potential induced at z by the source distribution on the wall, by the uniform stream and by the image vorticity. $W_1(z)$ is given by

$$w(z,t) = \frac{\aleph}{2\pi\mathrm{i}} \ln\sin\left(\frac{\pi}{\Lambda}(z - z_\mathrm{v}^*)\right) + w_\mathrm{s}(z) + U_0 z + \text{constant}, \tag{A 6}$$

where $w_\mathrm{s}(z)$ is given by (2.3) with $C_n(t)$ given by (A 6).

REFERENCES

Falco, R. 1991 A coherent structure model of the turbulent boundary-layer and its ability to predict Reynolds-number dependence. *Phil. Trans. R. Soc. Lond.* A **336**, 103–129.

Ince, E. L. 1956 *Ordinary Differential Equations*. Dover.

Lamb, H. 1932 *Hydrodynamics*. Cambridge University Press.

Smith, C. R., Walker, J. D. A., Haidari, A. H. & Sobren, U. 1991 On the dynamics of near-wall turbulence. *Phil. Trans. R. Soc. Lond.* A **336**, 131–175.

Walker, J. D. A. 1978 The boundary layer due to rectilinear vortex. *Proc. R. Soc. Lond.* A **359**, 167–188.

Uzkan, T. & Reynolds, W. C. 1967 A turbulent boundary layer on a wall moving at the free-stream velocity. *J. Fluid Mech.* **28**, 803–821.